Direct Observation of the Aharonov-Casher Phase

M. König,[1] A. Tschetschetkin,[1] E. M. Hankiewicz,[2,3] Jairo Sinova,[2] V. Hock,[1] V. Daumer,[1] M. Schäfer,[1] C. R. Becker,[1] H. Buhmann,[1] and L. W. Molenkamp[1]

[1]*Physikalisches Institut (EP 3), Universität Würzburg, Am Hubland, 97074 Würzburg, Germany*
[2]*Department of Physics, Texas A&M University, College Station, Texas 77843-4242, USA*
[3]*Department of Physics and Astronomy, University of Missouri, Columbia, Missouri 65211, USA*

(Received 17 August 2005; published 24 February 2006)

Ring structures fabricated from HgTe/HgCdTe quantum wells have been used to study Aharonov-Bohm type conductance oscillations as a function of Rashba spin-orbit splitting strength. We observe nonmonotonic phase changes indicating that an additional phase factor modifies the electron wave function. We associate these observations with the Aharonov-Casher effect. This is confirmed by comparison with numerical calculations of the magnetoconductance for a multichannel ring structure within the Landauer-Büttiker formalism.

DOI: 10.1103/PhysRevLett.96.076804 PACS numbers: 73.23.−b, 03.65.Vf, 71.70.Ej

In the early 1980s it was shown that a quantum mechanical system acquires a geometric phase for a cyclic motion in parameter space. This geometric phase under adiabatic motion is called the Berry phase [1], while its later generalization to include nonadiabatic motion is known as the Aharonov-Anandan phase [2]. A manifestation of the Berry phase is the well-known Aharonov-Bohm (AB) phase [3] of an electrical charge which cycles around a magnetic flux. Aside from the AB effect, the first experimental observation of the Berry phase was reported in 1986 for photons in a wound optical fiber [4]. Another important Berry phase effect is the Aharonov-Casher (AC) effect [5], which has been proposed to occur when an electron propagates in a ring structure in an external magnetic field perpendicular to the ring plane in the presence of spin orbit (SO) interaction [6].

This AC effect can be seen when two partial waves move around the ring in different directions. They will acquire a phase difference which depends on the spin orientation with respect to the total magnetic field $\vec{B}_{\mathrm{tot}} = \vec{B} + \vec{B}_{\mathrm{eff}}$ and the path of each partial wave. $\vec{B}_{\mathrm{eff}}$ is the effective field induced by the SO interaction. The phase difference is approximately [6]

$$\Delta\varphi_{\psi_s^+ - \psi_s^-} = -2\pi\frac{\Phi}{\Phi_0} - b\pi(1-\cos\theta) \qquad (1)$$

$$\Delta\varphi_{\psi_s^+ - \psi_{\bar{s}}^-} = -2\pi\frac{\Phi}{\Phi_0} - b2\pi r\frac{m^*\alpha}{\hbar^2}\sin\theta, \qquad (2)$$

where $s = \uparrow$ and $\downarrow$ denote parallel and antiparallel orientation to $\vec{B}_{\mathrm{tot}}$, $b = +1$ for $s = \uparrow$ and $b = -1$ for $s = \downarrow$, and the superscript $-(+)$ denotes a clockwise (counterclockwise) evolution, respectively. In the above equations, α is the SO parameter, r the ring radius, m^* the effective electron mass, and θ the angle between the external ($\vec{B}$) and the total magnetic field $\vec{B}_{\mathrm{tot}}$. For both equations, the first term on the right-hand side can be identified with the AB phase and the second term of Eq. (1) with the geometric Berry or Aharonov-Anandan phase. The second term in Eq. (2) represents the dynamic part of the AC phase, i.e., the phase of a particle with a magnetic moment that moves around an electric field. From the expressions above, it can be seen that an increase of α will lead to a phase change that increases continuously, whereas the contribution due to the geometric phase results in a phase shift limited to $\Delta\varphi_{\mathrm{geom}} \leq \pi$.

Both the AC phase [7] and the geometric phase [8,9] depend on the SO interaction. As a result, one expects a complicated nonmonotonic interference pattern as a function of magnetic field and SO interaction strength. So far, to our knowledge, apart from the AB effect no direct observation of phase-related effects in solid state systems has been reported. Recently, side bands in the Fourier transform of AB oscillations have been interpreted as an indication for the existence of a Berry phase [10–12]. However, these interpretations have been questioned [13–15]. Spin interference signals in square loop arrays have been reported recently by Koga *et al.* [16] but their direct relationship to the AC effect is not easily established. It thus would be important to observe these phase-related effects directly.

Here, we present experimental results on the magnetotransport properties of a HgTe ring structure. The strength of the SO interaction is controlled via a gate electrode by varying the asymmetry of the quantum well structure. We observe systematic variations in the conductance of the device as a function of both external B field and gate voltage. The gate-voltage dependent oscillations clearly exhibit a nonmonotonic phase change, which is related to the dynamic part of the AC phase. This interpretation is confirmed by numerical calculations for multichannel rings within the Landauer-Büttiker formalism. The effects discussed here are observed in several samples of various dimensions. For clarity, we present only data obtained from one sample.

The samples are fabricated on type-III HgTe/HgCdTe quantum well (QW) structures with electron mobilities of the order of 10^5 cm^2/(V s). This narrow-gap material exhibits a strong Rashba spin-orbit (SO) splitting [17], which can be modified over a wide range via an externally applied gate voltage [18,19]. The n-type QWs are symmetrically modulation doped and have been grown by molecular beam epitaxy [18,20]. The width of the HgTe-QW is 12 nm. The device structure is fabricated by optical and e-beam lithography and wet chemical etching [21]. A picture of the sample is shown in Fig. 1. The width of the leads in each arm of the ring is 300 nm and the ring radius is 1 μm. Directly attached to the ring is a Hall bar. Both components, ring and Hall bar, are covered by an insulator (Si_3N_4) and a metal gate electrode (Au). Because of these layers, the structure becomes asymmetric and a nonzero Rashba splitting is found for $V_{\mathrm{Gate}} = 0$. For all measurements, the samples were mounted in a ^{3}He/^{4}He dilution cryostat with a base temperature of $\sim$20 mK.

An applied gate voltage leads to a change in carrier concentration, electron mobility, and the Rashba SO splitting energy (Δ_R). These sample parameters were deduced directly from magnetotransport measurements of the attached Hall bar structure (see Fig. 1). The Rashba SO splitting energy of the presented sample could be varied from zero up to $\Delta_R \approx 6$ meV. These values are obtained by analyzing the Fourier transform of the Shubnikov–de Haas (SdH) oscillations. The Rashba splitting energy depends linearly on the applied gate voltage for $-4\ \mathrm{V} \leq V_{\mathrm{Gate}} \leq 0\ \mathrm{V}$. In this range the carrier concentration changes linearly between 1.85×10^{12} and 2.21×10^{12} cm^{-2}. An estimation for the symmetry point, $\Delta_R = 0$, yields $V_{\mathrm{Gate}} \approx (-2.57 \pm 0.02)$ V [Fig. 1(a)]. The AB oscillations for this gate voltage are displayed in Fig. 1(b). The period of 1.3 mT is consistent with the ring radius of $r = 1$ μm. Figure 2 shows a more detailed gate-voltage dependent magnetoconductance. For the displayed gate-voltage range, the change of carrier density is negligible. Here, two regions can clearly be distinguished. Near the symmetry point, there is no noticeable influence of the SO coupling on the position of the conductance oscillations [Fig. 3(a)]. The symmetry point of $V_{\mathrm{Gate}} = -2.568$ V has been determined from Fig. 2.

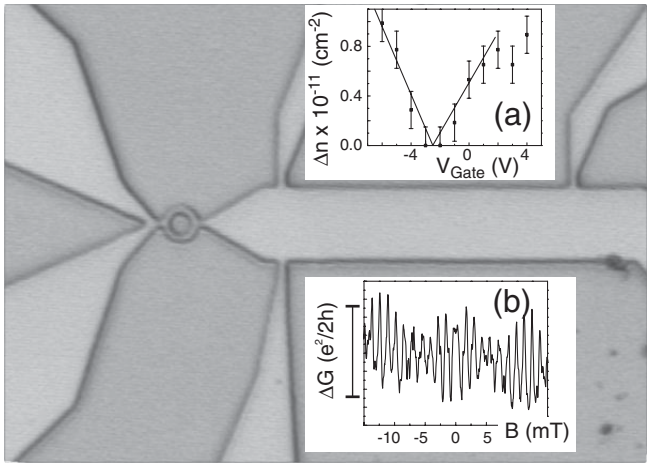

FIG. 1. Microscope image of the sample layout without top gate electrode. The average ring radius is 1 μm and the width of each arm is 300 nm. Inset (a): the symmetry point is estimated from the subband population differences as a function of the applied gate voltage, i.e., $V_{\mathrm{Gate}} \approx -2.57$ V. Inset (b) shows the conductance oscillations at $V_{\mathrm{Gate}} = -2.57$ V. The period, $\Delta B = 1.3$ mT, is consistent with the ring radius.

For increasing Δ_R the situation is drastically modified. Over a large range in gate voltage which corresponds to Δ_R from zero up to $\sim$150 μeV, the AB oscillations show phase shifts and bifurcations with increasing gate voltage (Fig. 2). A repetitive sequence of maxima and minima can be observed. Qualitatively, the observed conductance fluctuations represent the expected interference pattern due to phase differences for different spin orientation of the partial waves propagating around the ring [cf. Eqs. (1) and (2)]. The phase differences are caused by the change in strength of the SO coupling and thus the orientation of the total magnetic field with respect to the ring plane. The oscillations are symmetric in magnetic field and with respect to the applied gate voltage around the symmetry value of $V_{\mathrm{Gate}} = -2.568$ V. This behavior is expected for the SO coupling controlled dynamic part of the AC phase. In contrast, the geometric phase contribution to Eq. (1) varies only slowly with increasing SO interaction, so that one does not anticipate a discernible signature of this effect for the gate-voltage range studied here.

To verify that the experimental data represent a direct observation of the Aharonov-Casher phase in multichannel rings, we compare them to numerical calculations within the Landauer-Büttiker (LB) formalism [22]. The effective mass Hamiltonian for a two-dimensional ring with Rashba

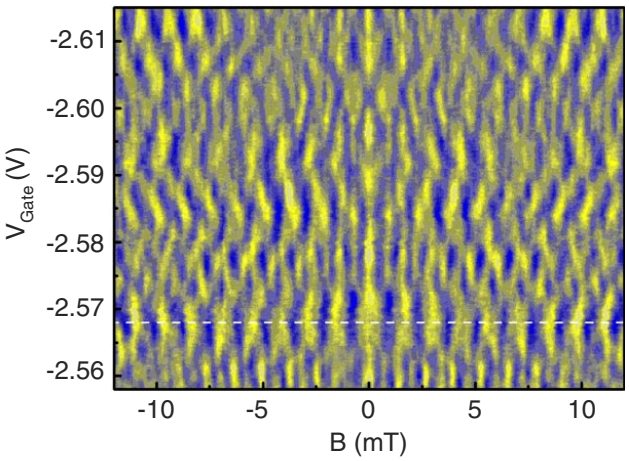

FIG. 2 (color online). Color plot of the conductance fluctuations, maxima (yellow) and minima (blue), as a function of magnetic field and gate voltage. The dashed line indicates $\Delta_R = 0$ which can be located at $V_{\mathrm{Gate}} = -2.568$ V, based on the mirror symmetry of the conductance around this line.

SO interaction and in a perpendicular magnetic field, B_z, is given by:

$$\hat{H}_r = \frac{\hat{\pi}^2}{2m^*} + \frac{\alpha}{\hbar}(\hat{\sigma} \times \hat{\pi})_z + \hat{H}_Z + \hat{H}_{\text{conf}}(r) + \hat{H}_{\text{dis}}, \quad (3)$$

where $\hat{\pi} = \hat{\mathbf{p}} - e\hat{\mathbf{A}}$ and $\hat{H}_Z = \frac{1}{2} g \mu_B \sigma_z B_z$. The first term is the kinetic energy contribution, the second term corresponds to the spin-orbit Rashba interactions, the third is the Zeeman interaction, and $\hat{H}_{\text{conf}}$ and $\hat{H}_{\text{dis}}$ are the confinement and disorder components of the Hamiltonian, respectively. For an ideal 1D ring, the conductance in the magnetic and Rashba fields can be found analytically [6,23–25]. However, our actual experimental structures are not 1D and multichannel effects have to be taken into account. Here, we use the concentric tight-binding (TB) approximation to model the multichannel rings extending the calculations in Ref. [22]. Within this approximation, the Hamiltonian, which is not only including the Rashba interactions but also the effect of magnetic field, becomes:

$$\begin{aligned}\hat{H}_r = & \sum_{n,m=1}^{N,M} \sum_{\sigma=\uparrow,\downarrow} \epsilon_{nm} c^\dagger_{nm,\sigma} c_{n,m,\sigma} \\ & - \sum_{n,m=1}^{N,M} \sum_{\sigma=\uparrow,\downarrow} [t_\Theta^{n,n+1,m} e^{i\Phi r_m/\Phi_0} c^\dagger_{nm,\sigma} c_{n+1,m,\sigma'} + \text{H.c.}] \\ & - \sum_{n=1}^{N} \sum_{m=1}^{M-1} \sum_{\sigma=\uparrow,\downarrow} [t_r^{m,m+1,n} c^\dagger_{nm,\sigma} c_{n,m+1,\sigma'} + \text{H.c.}], \quad (4)\end{aligned}$$

where n and m designate the sites in the azimuthal (Θ) and radial directions (r), respectively; $\epsilon_{nm} = 4t\sigma_0 - \frac{1}{2} g \sigma_z \mu_B B_z$ is the on-site energy where $t = \hbar^2/(2m^* a^2)$ and a is the lattice constant along the radial direction. $t_\Theta^{n,n+1,m}$ and $t_r^{m,m+1,n}$ are matrices describing generalized (with the inclusion of spin-orbit interactions) the nearest neighbor hopping energies in azimuthal and radial directions, respectively [22]. In the Landau gauge, the hopping parameter in azimuthal direction is modified through the term $e^{i\Phi r_m/\Phi_0}$, where $\Phi = \pi B_z a$, $\Phi_0 = h/e$, and $r_m = r_1 + (m-1)a$ is the radius of a ring with m modes in radial direction. The innermost ring radius corresponds to $m = 1$ while $m = M$ stands for the outermost ring radius. We also assume that the lattice spacing along the azimuthal direction in the outermost ring is the same as that in the radial direction. The ring is attached to two semi-infinite, paramagnetic leads that constitute reservoirs of electrons at chemical potentials μ_1 and μ_2. The influence of semi-infinite leads in the mesoscopic regime is taken into account through the self-energy term and the total charge conductance is calculated as outlined in Ref. [22].

We use an effective electron mass of $m^* = 0.031 m_0$ and effective g factor $|g| = 20$ in accordance with n-doped HgTe-QW parameters [26]. To verify the experimentally determined zero value of SO interaction at $V_{\text{Gate}}(\Delta_R = 0) = -2.568$ V we have calculated the conductance of a

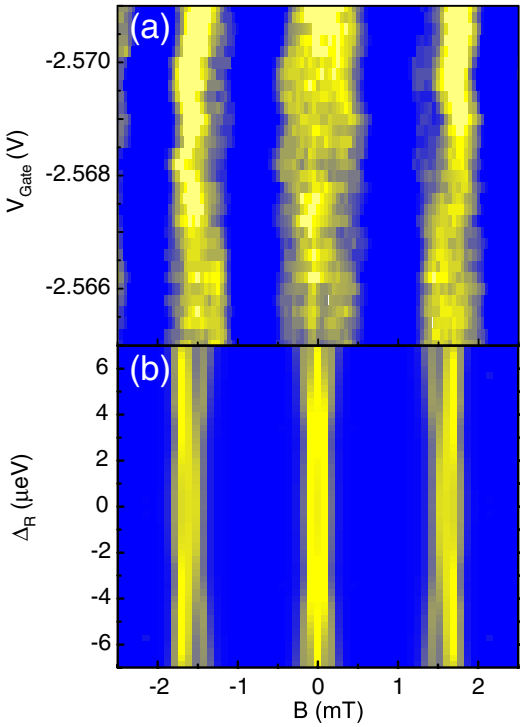

FIG. 3 (color online). (a) Near the symmetry point ($V_{\text{Gate}} = -2.568$ V) the interference pattern is unperturbed by the SO interaction. (b) The theoretical calculations for a 6-channel ring show consistent results for the corresponding range of Δ_R. Yellow and blue correspond to conductance maxima and minima, respectively.

6-channel ring within the LB formalism. Figure 3(b) shows the calculated conductance as a function of Rashba energy and magnetic field. We have found that for small Rashba energies, less than 5 μeV, the interference pattern is almost unperturbed by SO interactions and displays the multichannel Aharonov-Bohm oscillations, similar to the experimental data [see Fig. 3(a)]. Furthermore, a comparison of the experimental and the theoretical data leads to the conclusion that a change in the gate voltage of 10 mV leads to a change of 35 μeV in the Rashba energy, which is in good agreement with the results obtained from the Shubnikov–de Haas oscillations.

To verify the existence of AC phase, we performed the conductance calculations for much larger Rashba couplings. In the case of a strictly 1D ring, the appearance of the AC phase leads to periodic oscillations in conductance as a function of the Rashba energy [24,25]. In contrast, the theoretically predicted interference pattern for conductance is more complex for a multichannel ring. In this case, the repetitive conductance minima and maxima move diagonally as a function of SO coupling, as can be seen in the theoretical simulation [Fig. 4(b)]. For this calculation a ring with six channels was assumed (in agreement with an experimental estimate), where only one channel is conducting coherently. This latter assump-

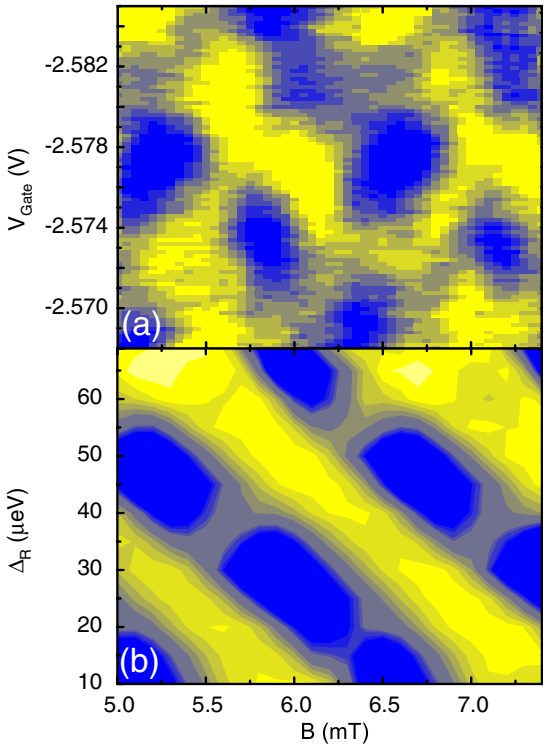

FIG. 4 (color online). When the SO interaction is modified via the gate voltage, a shift of the conductance maxima (yellow) can be observed due to the Aharonov-Casher phase (a). In (b), the theoretical results for the conductance in a 6-channel ring as a function of the Rashba energy and B_{ext} are shown. The scaling of the y axis allows a direct comparison of the experimental and theoretical data.

tion is corroborated by the experimental results. For more than one coherent channel, the interference pattern would be much more complex and smeared out. The distinct interference pattern is a strong indication that there is only one coherent conducting channel, presumably because of impurities and imperfections in the ring geometry. Additional incoherent conductance paths contribute mainly to the nonoscillating background, so that their effect on the interference pattern is negligible. The theoretical model reproduces the main features of experimental data, i.e., the diagonal position of conductance maxima and minima [Fig. 4(a)]. A more quantitative comparison of the experimental and theoretical data is difficult and should take into account incoherence effects as well as the change in width of the ring which is cumbersome to estimate.

In conclusion, we have measured the transport properties of HgTe ring structures with a continuously adjustable SO interaction. In these structures, the AB-type magnetoconductance oscillations exhibit significant phase changes when the Rashba SO splitting energy is varied. A numerical analysis shows that these fluctuations are a direct consequence of an Aharonov-Casher phase contribution to the electronic wave function. Thus, the experimental results provide the first direct observation of the Aharonov-Casher effect.

We thank H.-A. Engel and D. Loss for useful discussions. The financial support of the Deutsche Forschungsgemeinschaft (SFB 410) and ONR (04PR03936-00 and N000140610122) is gratefully acknowledged.

[1] M. Berry, Proc. R. Soc. Lond. A **392**, 45 (1984).
[2] Y. Aharonov and J. Anandan, Phys. Rev. Lett. **58**, 1593 (1987).
[3] Y. Aharonov and D. Bohm, Phys. Rev. **115**, 485 (1959).
[4] A. Tomita and R. Y. Chiao, Phys. Rev. Lett. **57**, 937 (1986).
[5] Y. Aharonov and A. Casher, Phys. Rev. Lett. **53**, 319 (1984).
[6] J. Nitta, F. E. Meijer, and H. Takayanagi, Appl. Phys. Lett. **75**, 695 (1999).
[7] H. Mathur and A. D. Stone, Phys. Rev. Lett. **68**, 2964 (1992).
[8] A. G. Aronov and Y. B. Lyanda-Geller, Phys. Rev. Lett. **70**, 343 (1993).
[9] T. Z. Qian and Z. B. Su, Phys. Rev. Lett. **72**, 2311 (1994).
[10] A. F. Morpurgo, J. P. Heida, T. M. Klapwijk, B. J. van Wees, and G. Borghs, Phys. Rev. Lett. **80**, 1050 (1998).
[11] J. B. Yau, E. P. De Poortere, and M. Shayegan, Phys. Rev. Lett. **88**, 146801 (2002).
[12] M. J. Yang, C. H. Yang, and Y. B. Lyanda-Geller, Europhys. Lett. **66**, 826 (2004).
[13] H. De Raedt, Phys. Rev. Lett. **83**, 1700 (1999).
[14] A. G. Mal'shukov and K. A. Chao, Phys. Rev. Lett. **90**, 179701 (2003).
[15] A. G. Wagh and V. C. Rakhecha, Phys. Rev. Lett. **90**, 119703 (2003).
[16] T. Koga, Y. Sekine, and J. Nitta, cond-mat/0504743.
[17] E. I. Rashba, Fiz. Tverd. Tela **2**, 1224 (1960) [Sov. Phys. Solid State **2**, 1109 (1960)]; Y. A. Bychkov and E. I. Rashba, J. Phys. C **17**, 6039 (1984).
[18] X. C. Zhang, A. Pfeuffer-Jeschke, K. Ortner, V. Hock, H. Buhmann, C. R. Becker, and G. Landwehr, Phys. Rev. B **63**, 245305 (2001).
[19] Y. S. Gui, C. R. Becker, N. Dai, J. Liu, Z. J. Qiu, E. G. Novik, M. Schäfer, X. Z. Shu, J. H. Chu, H. Buhmann, and L. W. Molenkamp, Phys. Rev. B **70**, 115328 (2004).
[20] F. Goschenhofer, J. Gerschütz, A. Pfeuffer-Jeschke, R. Hellmig, C. R. Becker, and G. Landwehr, J. Electron. Mater. **27**, 532 (1998).
[21] V. Daumer, I. Golombek, M. Gbordzoe, E. G. Novik, V. Hock, C. R. Becker, H. Buhmann, and L. W. Molenkamp, Appl. Phys. Lett. **83**, 1376 (2003).
[22] S. Souma and B. K. Nikolic, Phys. Rev. B **70**, 195346 (2004).
[23] F. E. Meijer, A. F. Morpurgo, and T. M. Klapwijk, Phys. Rev. B **66**, 033107 (2002).
[24] D. Frustaglia and K. Richter, Phys. Rev. B **69**, 235310 (2004).
[25] B. Molnar, F. M. Peeters, and P. Vasilopoulos, Phys. Rev. B **69**, 155335 (2004).
[26] X. C. Zhang, K. Ortner, A. Pfeuffer-Jeschke, C. R. Becker, and G. Landwehr, Phys. Rev. B **69**, 115340 (2004).